Journal of Environmental Chemical Engineering 14 (2026) 124441

Contents lists available at ScienceDirect

Journal of Environmental Chemical Engineering

journal homepage: www.elsevier.com/locate/jece

Assessing the photochemical lifetimes of the sulfonamide antibiotic sulfamethoxazole, of significance for sunlit freshwaters

Sara Abdelli [a,b], Luca Carena [a], Enmanuel Cruz Muñoz [c], Davide Ballabio [c], Viviana Consonni [c], Roberto Todeschini [c], Javier Marugán [d,e], Ángela García-Gil [f], Paola Calza [a], Laura Ferrando-Climent [b], Davide Vione [a,*]

[a] Dipartimento di Chimica, Università di Torino, Via Pietro Giuria 5, Torino 10125, Italy
[b] Tracer Technology Department, Environmental Technology Section, Institute for Energy Technology, Instituttveien 18, Kjeller 2007, Norway
[c] Department of Earth and Environmental Sciences, University of Milano-Bicocca, Piazza della Scienza, 1, Milano 20126, Italy
[d] Grupo de Ingeniería Química y Ambiental, Universidad Rey Juan Carlos, ESCET, C. Tulipán s/n, Móstoles, Madrid 28933, Spain
[e] Instituto de Investigación de Tecnologías para la Sostenibilidad, Universidad Rey Juan Carlos, ESCET, C. Tulipán s/n, Móstoles, Madrid 28933, Spain
[f] Process Design, Repsol Technology Lab, Móstoles, Madrid 28935, Spain

ARTICLE INFO

Keywords:
Photochemical reactions
Direct photolysis
Sunlit surface waters
Pharmaceuticals
Self-depuration of natural waters

ABSTRACT

Photochemical modeling was used to evaluate the photodegradation kinetics of sulfamethoxazole (SMX) in sunlit natural freshwater environments, utilizing available data on SMX absorption spectrum, direct photolysis quantum yield, and second-order reaction rate constants with photochemically produced reactive intermediates (PPRIs). The anionic form of SMX is considered here, which prevails in the majority of surface-water conditions (pH > 5.6). SMX would be photodegraded quite rapidly in well-mixed waters under sunny weather, with direct photolysis serving as the predominant pathway in most cases. Among the water parameters, depth and the dissolved organic carbon (DOC) primarily influence the photodegradation of SMX, which would be faster in shallow waters with low DOC. This feature enabled the extension of SMX photochemical lifetime prediction to lakes located within the 60°S-60°N latitude belt, where data on DOC, water depth and sunlight irradiance are available. The fastest photodegradation of SMX (annual average) is expected in the tropical belt, where the combination of high irradiance and low DOC would be most favorable for direct photolysis. With fair weather and good water mixing, typical SMX lifetimes would range from days to some weeks depending on the specific conditions. The lifetimes predicted in shallow waters are consistent with several literature reports of SMX photodegradation kinetics in the laboratory.

1. Introduction

Pharmaceutical compounds are frequently detected in natural waters worldwide, and their presence raises concern because of their potentially adverse effects on aquatic biota and, in some cases, on human health due to the use of water for irrigation, recreational activities, and as source of drinking water. The main sources of pharmaceuticals in environmental waters are the discharge of incompletely treated urban and industrial wastewater, animal husbandry, and aquaculture [1]. Many pharmaceuticals are polar and poorly biodegradable, which helps them survive traditional wastewater treatment technologies so that they reach the natural environment through the wastewater discharge [2]. Antibiotics such as sulfamethoxazole raise additional concern, because their occurrence in the natural environment can promote the development of antimicrobial resistance in bacteria [1,3].

Once they reach natural waters, those pharmaceuticals that are biorecalcitrant are often not sufficiently biodegraded [1,4]; consequently, phototransformation may serve as a significant competing pathway for their attenuation [5]. Photodegradation processes occur through direct photolysis and indirect photochemistry. In direct photolysis, the pollutant absorbs sunlight and is consequently degraded. When indirect photochemistry occurs, sunlight is absorbed by natural compounds called photosensitizers (mainly nitrate, nitrite, and chromophoric dissolved organic matter or CDOM) to produce reactive transient species known as photochemically produced reactive intermediates (PPRIs) [6]. The main PPRIs in sunlit natural freshwaters

* Corresponding author.
E-mail address: davide.vione@unito.it (D. Vione).

https://doi.org/10.1016/j.jece.2026.124441
Received 27 March 2026; Received in revised form 22 June 2026; Accepted 1 August 2026
Available online 2 August 2026

are the hydroxyl ($^{\bullet}OH$) and carbonate ($CO_3^{\bullet-}$) radicals, singlet oxygen ($^1O_2$), and CDOM triplet states ($^3CDOM^*$). In natural waters, PPRIs reach low steady-state concentrations that result from the balance between photogeneration and scavenging/quenching. In particular: $^{\bullet}OH$ is scavenged by dissolved organic matter (DOM), and by HCO_3^- and CO_3^{2-} (in the latter two cases, to produce $CO_3^{\bullet-}$); $CO_3^{\bullet-}$ is scavenged by DOM; $^3CDOM^*$ are quenched by dissolved oxygen to partially produce $^1O_2$, and $^1O_2$ is quenched by water [5–8]. For these reasons, in addition to the irradiance and spectrum of sunlight, important environmental factors that affect contaminants photodegradation are the concentrations of NO_3^-, NO_2^-, HCO_3^-, CO_3^{2-} and the dissolved organic carbon (DOC), which measures DOM and correlates with CDOM. Water depth is also an important factor, because shallow waters are more thoroughly illuminated than deep waters, the lower depths of which are often in the dark [6].

Sulfamethoxazole (SMX) is a widely used sulfonamide antibiotic that is frequently detected in natural surface waters at ng L^{-1} – μg L^{-1} levels [9]. Photodegradation is thought to play an important role in the environmental attenuation of SMX. However, contrasting evidence exists regarding its photolability [10–13]. Although several results indicate that SMX may undergo rapid photodegradation at the laboratory scale [11–13], these experiments may not be representative of natural environmental conditions.

Recently, a complete set of photoreactivity parameters has been measured for SMX [14], enabling modeling of its environmental photodegradation. Photochemical models can be very useful for bridging the gap between irradiation experiments (which are often limited by the need to use very shallow water columns, where photoreactions tend to be fast) and the natural environment [15], which is often characterized by much deeper water columns among other factors.

On this basis, the present work aims to assess the photochemical persistence of SMX through modeling. Specifically, the work aims to:

(i) examine how various environmental factors, such as NO_3^-, NO_2^-, HCO_3^-, CO_3^{2-}, DOC and water depth affect SMX degradation, identifying which are the most influential;
(ii) assess the photochemical lifetimes of SMX across different geographic regions.

The goal is to understand the photochemical persistence of SMX under conditions typical of natural water environments. Whenever possible, the model predictions were compared to outcomes from irradiation experiments available in the literature.

2. Methods

2.1. Prediction of mid-latitude lifetimes and transformation pathways of SMX

The photodegradation kinetics and pathways of SMX that are significant for natural surface waters were initially predicted under summer irradiation conditions using the APEX software (Aquatic Photochemistry of Environmental Xenobiotics). This software predicts phototransformation of contaminants in a well-mixed water column based on photochemically relevant data, including absorption spectra, direct photolysis quantum yields, second-order reaction rate constants with PPRIs, and environmental features. The latter include water depth, chemistry (values of photochemically relevant parameters: DOC, $[NO_3^-]$, $[NO_2^-]$, $[HCO_3^-]$, $[CO_3^{2-}]$), and water absorption spectra. By default, APEX assumes fair-weather summertime irradiation (mid-July, mid-latitude) [16].

In the case of SMX, the used values of direct photolysis quantum yield and second-order reaction rate constants with PPRIs are shown in Table 1. The absorption spectrum of SMX is reported in Fig. 1, where it is compared with the default spectrum of sunlight used by APEX [14,16]. The reported parameters are relevant to the anionic form of SMX, which prevails over neutral SMX at pH > 5.6 [12], that is, in the majority of natural waters. There is evidence that the direct photolysis of neutral SMX is faster compared to anionic SMX [12].

Table 1
Photochemical reactivity parameters for the anionic form of SMX [14]: photolysis quantum yield Φ and second-order reaction rate constants k with PPRIs. The reaction between SMX and $^1O_2$ is very slow [17].

Variable & measure unit	Value
Φ_{SMX}, mol E^{-1}	2.9×10^{-2}
$k_{SMX,^{\bullet}OH}$, L mol^{-1} s^{-1}	2.73×10^{10}
$k_{SMX,CO_3^{\bullet-}}$, L mol^{-1} s^{-1}	1.02×10^{8}
$k_{SMX,^3CDOM^*}$, L mol^{-1} s^{-1}	1.41×10^{8} (*)
$k_{SMX,^1O_2}$, L mol^{-1} s^{-1}	$< 10^{5}$

(*) Due to a phenomenon called back-reduction by the antioxidant moieties of DOM [18] (*vide infra*), this rate constant should be multiplied by $\psi = 1 / (1 + DOC/[DOM]_{½})$, where $[DOM]_{½} = 1.3$ mgC L^{-1} (average value).

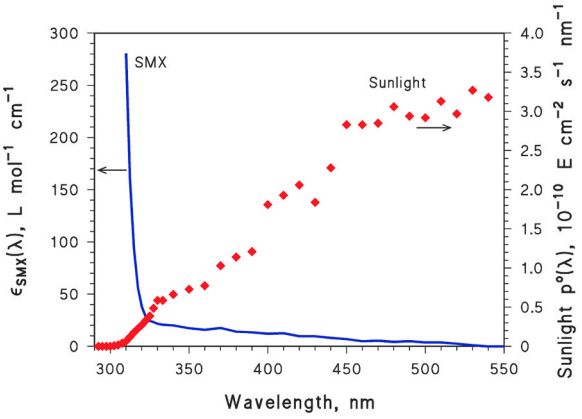

Fig. 1. Left Y-axis: absorption spectrum of SMX (molar absorption coefficient $\varepsilon_{SMX}(\lambda)$). Right Y-axis: sunlight spectrum (spectral photon flux density $p^{\circ}(\lambda)$).

APEX assumes that the photosensitizers (CDOM, nitrate, and nitrite) absorb sunlight and produce the relevant PPRIs ($^{\bullet}OH$, $^1O_2$, $CO_3^{\bullet-}$ and $^3CDOM^*$). At the same time, the contaminant absorbs sunlight and undergoes direct photolysis. Sunlight absorption rate by contaminants and photosensitizers is computed by taking into account the competition for absorption in a medium where several species are able to absorb radiation [16]:

$$P_{a,C} = 10 \int_{\lambda} \left[\frac{\varepsilon_C(\lambda) C_C}{A_1(\lambda) DOC} \frac{p^{\circ}(\lambda)}{d} \left(1 - 10^{-100 A_1(\lambda) DOC d}\right) \right] d\lambda \quad (1)$$

Where $P_{a,C}$ [E L^{-1} s^{-1}] (1 E = 1 Einstein = 1 mol of photons) is the solar photon flux absorbed by the compound C (contaminant or photosensitizer), $\varepsilon_C(\lambda)$ [L mol^{-1} cm^{-1}] is the molar absorption coefficient of C at the wavelength λ, C_C [mol L^{-1}] is the concentration of C, $A_1(\lambda)$ [L mgC^{-1} cm^{-1}] is the absorbance of water over an optical path length of 1 cm per unit DOC, $p^{\circ}(\lambda)$ [E cm^{-2} s^{-1} nm^{-1}] is the solar spectral photon flux density incident over the water column, d [m] is water depth, 10 is the conversion factor between [cm^{-2} m^{-1}] and [L^{-1}], and 100 is the conversion factor between [m] and [cm].

When the absorbance $A_1(\lambda)$ is not available for a given water body, it is assumed $A_1(\lambda) = 0.45\ e^{-0.015\ \lambda}$ as a reasonable approximation [6,16]. Note that water absorbance in the spectral region 280–500 nm, which is most relevant to the photodegradation of contaminants, is mostly accounted for by CDOM. Therefore, if C = CDOM, it is assumed that $\varepsilon_C(\lambda)\ C_C = A_1(\lambda)$ DOC in Eq. (1) [16].

When C = contaminant (SMX in the present case), $C_C = C_{SMX}$ is assumed to be very low (sub-nM) as per typical environmental

conditions, and the kinetics of direct photolysis is computed as $k_{SMX,d.p.} = \Phi_{SMX}\, P_{a,SMX}\, C_{SMX}^{-1}$, where $k_{SMX,d.p.}$ is the first-order rate constant of direct photolysis (measure unit of [time^{-1}]) and Φ_{SMX} is the direct photolysis quantum yield (Table 1) [16].

When C = photosensitizer, the formation rate of the PPRI ($^{\bullet}OH$, $^1O_2$, or $^3CDOM^*$) is calculated as $R_{PPRI} = \Phi_{PPRI}\, P_{a,C}$, where Φ_{PPRI} is the quantum yield of PPRI photogeneration from the irradiated photosensitizer. The relevant steady-state concentration is [PPRI] = $R_{PPRI}\, k_{decay}^{-1}$, where k_{decay} is a pseudo-first order rate constant that considers PPRI scavenging or quenching [16].

The case of $CO_3^{\bullet-}$ is a bit different, because this PPRI is generated by $^{\bullet}OH$ and $^3CDOM^*$ and scavenged by DOM [5,6]:

$$^{\bullet}OH + HCO_3^- \rightarrow H_2O + CO_3^{\bullet-} \quad [k_2 = 8.5\times 10^6\ L\ mol^{-1}\ s^{-1}] \tag{2}$$

$$^{\bullet}OH + CO_3^{2-} \rightarrow OH^- + CO_3^{\bullet-} \quad [k_3 = 3.9\times 10^8\ L\ mol^{-1}\ s^{-1}] \tag{3}$$

$$^3CDOM^* + CO_3^{2-} \rightarrow CDOM^{\bullet-} + CO_3^{\bullet-} \quad [k_4 = 10^6\ L\ mol^{-1}\ s^{-1}] \tag{4}$$

$$CO_3^{\bullet-} + DOM \rightarrow CO_3^{2-} + DOM^{\bullet+} \quad [k_5 = 10^2\ L\ mg_C^{-1}\ s^{-1}] \tag{5}$$

In this case, the steady-state concentration is calculated as follows:

$[CO_3^{\bullet-}] = \{[^{\bullet}OH]\,(k_2\,[HCO_3^-] + k_3\,[CO_3^{2-}]) + k_4\,[^3CDOM^*]\,[CO_3^{2-}]\}\,(k_5\,DOC)^{-1}$.

Degradation kinetics of SMX upon reaction with each PPRI are formulated as [19]:

$$k_{SMX(PPRI)} = k_{SMX,PPRI}\,[PPRI] \tag{6}$$

Where $k_{SMX(PPRI)}$ is a first-order photodegradation rate constant and $k_{SMX,PPRI}$ is the second-order rate constant for the reaction between SMX and the PPRI (see Table 1 for the values of $k_{SMX,PPRI}$). In the case of $^3CDOM^*$, a multiplication factor $\psi = 1 / (1 + DOC/[DOM]_{½})$ should be included in Eq. (6) to account for the effect of DOM antioxidants on SMX photodegradation [18] (*vide infra* in Section 2.2). The overall first-order rate constant for SMX photodegradation (k_{SMX}) is the sum of the rate constants of all the separate photochemical processes, namely [16]:

$$k_{SMX} = k_{SMX,d.p.} + \sum_{PPRI} k_{SMX(PPRI)} \tag{7}$$

Once k_{SMX} is known, the corresponding half-life time can be obtained as $t_{½}(SMX) = \ln 2\ (k_{SMX})^{-1}$.

In this work, the half-life time of SMX was computed by APEX for different water chemistry and depth conditions, assuming fair-weather and mid-latitude summertime irradiation. Environmental parameters were made to span relatively wide intervals, thus DOC was varied within 0.1 – 10 mgC L^{-1}, nitrate within 10^{-5} – 10^{-3} mol L^{-1}, nitrite within 10^{-7} – 10^{-5} mol L^{-1}, bicarbonate within 10^{-4} – 10^{-2} mol L^{-1}, carbonate within 10^{-6} – 10^{-4} mol L^{-1}, and depth within 0.1 – 10 m. Deeper waters were not considered at this stage, to facilitate the comparison between model predictions and the available data from SMX irradiation experiments in natural water samples, where water depths were relatively low [10–13]. Model calculations yielded around 150,000 data points.

These data were structured in a matrix with 150,000 rows and 45 columns, where each column contained the values of the six independent variables (d, $[NO_3^-]$, $[NO_2^-]$, $[CO_3^{2-}]$, $[HCO_3^-]$, and DOC), their transformations to account for non-linear trends (e.g., x^2, x^3, log(x), 1-exp(-x)), and the dependent variable $t_{½}$(SMX) [20,21]. The 150,000 simulations were randomly divided into training (50%) and test (50%) sets. The simulations of the training set were used to establish model coefficients, and variables were selected on the basis of their standardized regression coefficients [22]: variables and transformations with negligible effect (low standardized coefficients) on the half-life were excluded and a regression model was calibrated again by considering only the retained variables, that is, d, DOC and some of their transformations. The model achieved excellent accuracy on training and test samples, with R^2 equal to 0.953 for both sets and RMSE (root mean squared error) equal to 0.254 in both cases.

2.2. Prediction of SMX lifetimes on a quasi-global scale (60°S – 60°N latitude belt)

Modeling the photodegradation of contaminants on a broad geographic scale relies on data of DOC, depth, and sunlight radiation intensity (spectral photon flux density $p^{\circ}(\lambda)$), which are available for global lakes [23–25]. The lack of global concentration data for nitrate, nitrite, carbonate, and bicarbonate prevents the $^{\bullet}OH$ and $CO_3^{\bullet-}$ reactions to be modeled. Furthermore, lack of worldwide pH data does not allow for acid-base equilibria of contaminants to be considered.

Therefore, only the direct photolysis and the indirect photoreactions triggered by $^3CDOM^*$ and $^1O_2$ can be taken into account [26,27], and only anionic SMX is modeled that is the prevalent form in most natural surface waters. Excluding the $^1O_2$ pathway that is irrelevant for SMX [14], the direct photolysis and the $^3CDOM^*$ reaction can be included in photochemical modeling. Furthermore, as shown later on, $^3CDOM^*$ reactions and especially the direct photolysis account for most of SMX photodegradation. On this basis, the pseudo-first order rate constant of SMX photodegradation was expressed as $k_{SMX} = k_{SMX,d.p.} + k_{SMX(^3CDOM^*)}$.

In the case of the $^3CDOM^*$ process, it is $k_{SMX(^3CDOM^*)} = \psi\, k_{SMX,^3CDOM^*}\,[^3CDOM^*]$. The values of ψ and $k_{SMX,^3CDOM^*}$ are shown in Table 1, while those of $[^3CDOM^*]$ are available for the global lakes included in the 60°S–60°N latitude belt [26]. Note that the term ψ accounts for the reduction of SMX intermediates back to the parent compound, carried out by the antioxidant moieties of DOM (AODOM, **reactions 8–10**) [18].

$$SMX + {}^3CDOM^* \rightarrow SMX^{\bullet+} + CDOM^{\bullet-} \tag{8}$$

$$SMX^{\bullet+} \rightarrow Products \tag{9}$$

$$SMX^{\bullet+} + AODOM \rightarrow SMX + AODOM^{\bullet+} \tag{10}$$

As far as the direct photolysis of SMX is concerned, quasi-global modeling is made possible by a monochromatic approximation. Typically, the absorption spectrum of a pollutant overlaps with the spectrum of sunlight over a range of wavelengths (290–550 nm in the case of SMX, see Fig. 1). However, it is almost always possible to find a single wavelength that approximates the behavior of the polychromatic system, with negligible loss in accuracy and considerable simplification of calculations [28].

The exact, polychromatic calculation of $k_{SMX,d.p.}$ is carried out as follows (note that the APEX software follows this same procedure [16]):

$$k_{SMX,d.p.} = \frac{10\ \Phi_{SMX}\,\tau}{d\ DOC}\int_{\lambda}\left[p^{\circ}(\lambda)\,\frac{\varepsilon_{SMX}(\lambda)}{A_1(\lambda)}\left(1-10^{-100\ A_1(\lambda)\ DOC\ d}\right)\right]d\lambda \tag{11}$$

Where $\tau = 2.1 \times 10^4$ is a conversion factor that takes into account the difference between the default irradiance of sunlight used in APEX and the year-averaged mid-latitude irradiance, at the same time converting between [s^{-1}] and [day^{-1}] units. Moreover, $\varepsilon_{SMX}(\lambda)$ is the molar absorption coefficient of SMX, Φ_{SMX} is reported in Table 1, and the other quantities have already been introduced when discussing Eq. (1).

The corresponding monochromatic equation (approximated) reads as follows [28]:

$$k_{SMX,d.p.} = \frac{10\ \eta_{SMX}\,\tau}{d\ DOC}\,p^{\circ}(\lambda_{eq})\,\frac{\varepsilon_{SMX}(\lambda_{eq})}{A_1(\lambda_{eq})}\left(1-10^{-100\ A_1(\lambda_{eq})\ DOC\ d}\right) \tag{12}$$

Where λ_{eq} is the 'equivalent monochromatic wavelength' that approximates the polychromatic system. Moreover, η_{SMX} is a photon efficiency, which replaces the quantum yield and accounts for the fact that the polychromatic irradiance of sunlight is much higher than the monochromatic irradiance at λ_{eq}. For this reason, η_{SMX} is expected to be much higher than Φ_{SMX} and, in general, the η values are not bound to be below 1 [28].

To find λ_{eq}, APEX was used to derive several $k_{SMX,d.p.}$ values with the

polychromatic Eq. (11), varying water depth and the DOC. Afterwards, such values were fitted with Eq. (12). Note that, once the wavelength is defined, the values of $p°(\lambda_{eq})$, $A_1(\lambda_{eq})$, and $\varepsilon_{SMX}(\lambda_{eq})$ are those used by APEX. From an operational point of view, such values are initially left as floating variables, together with η, and data fit typically yields $A_1(\lambda_{eq})$ as the most reliable result [28]. From the relationship $A_1(\lambda_{eq}) = 0.45 \exp(-0.015\ \lambda_{eq})$, the value of λ_{eq} is determined and a further fit is carried out, with fixed $[p°(\lambda_{eq}), A_1(\lambda_{eq}), \varepsilon_{SMX}(\lambda_{eq})]$ and with η as the only floating variable. By doing so, it is possible to derive all the parameters needed for Eq. (12).

At this stage, Eq. (12) holds for mid-latitude conditions. The extension of this equation to a quasi-global scale requires $p°(\lambda_{eq})$ to be generalized as a function of the day and latitude. To do so, the daily dose reaching the Earth's surface ($G_{day}(\lambda_{eq})$) was first computed as follows [29]:

$$G_{day}(\lambda_{eq}) = F_1\ p_{sn}°(\lambda_{eq})\ \tau_{DL} = \int_{1day} p°(\lambda_{eq}, t)\ dt \quad (13)$$

In Eq. (13), the values of the solar photon flux density at each hour of a given day, $p°(\lambda_{eq},t)$, were computed by introducing the zenith angle obtained with the Solar Position Algorithm (SPA) from the National Renewable Energy Laboratory (NREL) [30]. Moreover, the quantity $\tau_{DL} = \frac{2}{15}\arccos(-\tan(\varphi)\tan(\delta))$ is the day length in hours ([h day^{-1}] units; the value of the arccos is in degrees), with φ as the latitude and $\delta = 23.45° \sin\left(\frac{360}{365}(day + 284)\right)$ as the Sun's declination ($day = 1$ is 1st January and $day = 365$ is 31st December) [29]. Note that τ_{DL} can be obtained with the above expression only if $-60° < \varphi < 60°$, thus calculations are limited to the 60°S–60°N latitude belt. Furthermore, $p_{sn}°(\lambda_{eq})$ is the incident spectral photon flux density of sunlight at the solar noon, expressed as follows [31]:

$$p_{sn}°(\lambda_{eq}) = I_{AM0}(\lambda_{eq}) exp\left(\frac{-\kappa(\lambda_{eq})}{\cos(\varphi - \delta) + 0.506(96.08 + \varphi - \delta)^{-1.636}}\right)\frac{\lambda_{eq}}{hcN_a} \quad (14)$$

Where $I_{AM0}(\lambda_{eq})$ is the intensity of sunlight outside the atmosphere, $\kappa(\lambda_{eq})$ is the atmospheric extinction coefficient, h is Planck's constant, c is light's speed in vacuum, and N_a is Avogadro's number (for δ and φ, see definitions above). Note that the measure unit of λ_{eq} in the equation is [nm].

By so doing, it is possible to derive $F_1 = [p_{sn}°(\lambda_{eq})\ \tau_{DL}]^{-1} \int_{1\ day} p°(\lambda_{eq}, t)\ dt$ and to compute $G_{day}(\lambda_{eq})$ for all days in the year and for $-60° < \varphi < 60°$. Operationally, F_1 was initially derived for $\varphi = 45°$ and then it was checked that the value thus obtained could be applied in the whole latitude range $-60° < \varphi < 60°$. It was then possible to compute $p°(\lambda_{eq}) = F_1\ p_{sn}°(\lambda_{eq})$ for each day of the year, where $p°(\lambda_{eq})$ is the average photon flux density of sunlight on each given day. In this work, year averages of $p°(\lambda_{eq})$ were used in Eq. (12). In the same equation, it was used

$$\tau = (3600\ s\ h^{-1}) \times \tau_{DL} = 480 \arccos(-\tan(\varphi)\tan(\delta)) \text{ ([s day}^{-1}\text{] units).}$$

The data of $k_{SMX,d.p.}$ allowed for the calculation of $k_{SMX} = k_{SMX,d.p.} + k_{SMX(^3CDOM^*)}$ and of the SMX lifetime ($t_{½}(SMX) = \ln 2\ (k_{SMX})^{-1}$). The quasi-global maps of $t_{½}$(SMX) were obtained by means of the QGIS software (version 3.2.3-Bonn) [32]. For this purpose, the $t_{½}$(SMX) dataset was divided into four color-labeled groups, defined by considering the average (μ_y) and standard deviation (σ_y). In particular, the chosen intervals were: *(i)* $y < (\mu_y - \sigma_y)$; *(ii)* $(\mu_y - \sigma_y) < y < \mu_y$; *(iii)* $\mu_y < y < (\mu_y + \sigma_y)$, and *(iv)* $y > (\mu_y + \sigma_y)$. Reddish points indicate higher photochemical activity of lake water, while bluish points suggest lower photochemical activity.

2.2.1. The algebraic function to predict SMX lifetimes

The dataset was structured as a matrix comprising 72,380 rows (representing global lakes) and three primary columns: latitude, DOC, and depth. To enhance the model's predictive power, the dataset was augmented by incorporating non-linear transformations such as interaction terms and quadratic and cubic variables. Linear regression was used to model the relationship between these variables and the half-life time $t_{½}$(SMX). The dataset was split into two equal subsets: 50% for model training and 50% for independent testing.

The regression model yielded highly accurate predictions for both the training and test sets. Model performance was robust, achieving R^2 values of 0.994 for both sets, with Root Mean Squared Errors (RMSE) of 0.123 and 0.126, respectively.

2.2.2. Limitations of the photochemical model

The photochemical model used has limitations that stem partly from the approximations made and partly from the lack of more precise input data. First, water columns were assumed to be well mixed. Although the APEX model can handle stratified lakes, by considering the hypolimnion and epilimnion separately [33], no global data are currently available on thermocline depths, which vary during the year. Photoreactions are less efficient in stratified lakes than in mixed lakes, however [34]. For instance, assume a lake with $d = 40$ m, DOC = 3 mgC L^{-1}, and a thermocline depth of 20 m when it is stratified. Also, for simplicity, assume that epilimnion and hypolimnion have equal volumes. When water is well mixed, Eqs. (11,12) predict $k_{SMX,d.p.} = 4 \times 10^{-2}$ day^{-1} (summertime, fair weather, mid latitude). Under these circumstances, around 70% of the initial SMX would be degraded in one month in the whole lake, which would thus still contain ~30% of the initial SMX. When water is stratified, it is $k_{SMX,d.p.} = 8 \times 10^{-2}$ day^{-1} in the epilimnion, while practically no photodegradation occurs in the hypolimnion. In one month, ~90% of the initial SMX in the epilimnion would be degraded, but there would be negligible hypolimnion photodegradation. In these circumstances, the lake would contain ~55% of the initial SMX, mostly in the hypolimnion. SMX photodegradation would thus be more efficient in the mixed lake, despite the fact that photochemical reactions in the epilimnion of the stratified lake are faster than in the whole water column of the mixed lake. The difference between mixed and stratified lakes is larger if the hypolimnion volume is also larger, and in the case of fast photoreactions [9,33]. The latter circumstance, however, usually occurs in shallow lakes that are less likely to be stratified compared to deep lakes.

Water turbidity data are also not available globally, so the present model only considers absorption of sunlight. Suspended solids modify the underwater light field because they increase irradiance at the surface while decreasing it in deep water. However, if the whole water column is considered, as done here, the effect of solids is less substantial [35]. To minimize the impact of turbidity, very shallow lakes ($d < 5$ m) were excluded that are more likely to contain turbid water than deeper lakes [36]. These excluded lakes were the most numerous and followed the geographical distribution of the global lakes. Limited depth is conducive to fast photochemical reactions [5,6], but shallow lakes are also richer in DOC compared to deep ones [23]. According to Eqs. (11,12) the two parameters would partially offset each other in the direct photolysis of SMX, although, in general, shallow lakes are predicted to be more photoreactive environments [6], especially if their water is clear. Based on this selection criterion, the current estimate will provide a conservative assessment of the potential for SMX photodegradation in lake water.

Average spectral coefficients for organic matter were considered here with respect to $A_1(\lambda)$, since site-specific CDOM spectra are not available. The use of different coefficient values could affect the photoreactivity of CDOM [37], but that would be partially offset by the fact that strongly sunlight-absorbing CDOM is typically less photoreactive (with equal photon absorption) than weakly absorbing CDOM [38].

Ice cover during winter can significantly inhibit photoreactions [39]. To minimize this issue, lakes located above 500 m a.s.l. were excluded from this study as these are more likely to be covered with ice.

Finally, cloud cover decreases photoreaction rates compared to the clear-sky conditions considered here. The associated inhibition effect can reach up to 40–50% in some equatorial areas and in East Asia [40].

Despite the limitations mentioned above, this approach was able to predict the photochemical lifetime of clofibric acid in Lake Greifensee (Switzerland) within a factor of two [26,41], which is an excellent result for a model-based assessment.

3. Results and discussion

3.1. Mid-latitude lifetimes of SMX as a function of water chemistry and depth

The assessment of the influence of various water parameters on the photodegradation of SMX (see **Section 2.1**) suggested that NO_3^-, NO_2^-, HCO_3^-, and CO_3^{2-} would play a rather limited role, while DOC and the depth d would be very important. For this reason, Fig. 2 reports the half-life time of SMX as a function of DOC and d, showing that low values of these parameters favor photodegradation and yield lower $t_{½}$(SMX). Indeed, $t_{½}$(SMX) increases (i.e., photodegradation becomes slower) with increasing d and DOC. The negative effect of d on photodegradation is reasonable, because deep waters are typically poorly illuminated by sunlight [35]. Interestingly, for low d values that are representative of laboratory irradiation experiments conducted with SMX in natural water samples exposed to sunlight, Fig. 2 shows that $t_{½}$(SMX) would be in the hours-day range. This is the same range reported in several experimental studies [11–13]. To make a comparison, irradiation of SMX spiked to two different river waters under simulated sunlight yielded a lifetime of 1.6 summer sunny days (fair-weather, mid-July, mid-latitude) when the sample DOC was 3.1 mgC L^{-1}, and 1.4 summer sunny days when DOC = 5.5 mgC L^{-1} [12]. The APEX model predicts a lifetime of ~0.9 days (fair-weather, mid-July, mid-latitude as well) under the same DOC conditions and with cm-range water depth, mostly due to direct photolysis. Considering that irradiation experiments of SMX in ultra-pure water have yielded a lifetime of 0.8 days [12], a possible explanation for the difference between experiments and model predictions is a different degree of inhibition of SMX direct photolysis by the dissolved organic matter. Furthermore, note that the reported degree of agreement between experiments and predictions is very reasonable for a photochemical model.

The explanation of the DOC effect on $t_{½}$(SMX) (Fig. 2) requires consideration of the relative roles of different photoreaction pathways in the photodegradation of SMX. In most cases, the direct photolysis would account for over 90% of SMX photodegradation. An increase in the DOC inhibits direct photolysis reactions because high DOC means high CDOM, which competes with SMX for absorption of solar radiation and causes an increase of $t_{½}$(SMX) [35].

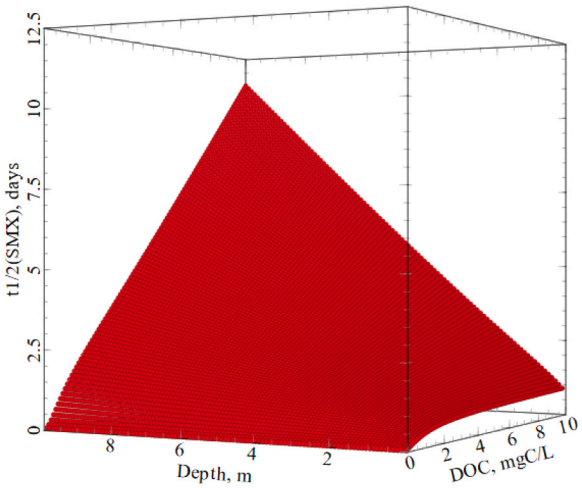

Fig. 2. Modeled values of the half-life time $t_{½}$(SMX), as a function of water depth and the DOC. Calculations were carried out with the APEX software and are referred to mid-latitude (45°N) and mid-July fair weather conditions.

Photochemical model calculations suggested that the roles of the different photoreaction pathways in SMX photodegradation would be as follows: direct photolysis > $CO_3^{\bullet-}$ > ^{3}CDOM* > $^\bullet$OH. Based on this, it is reasonable to extend the prediction of SMX photodegradation kinetics to a wide geographic scale. In such a case, only direct photolysis and ^{3}CDOM* reactions can be included [27], but direct photolysis alone accounts for most of SMX phototransformation.

An exception to the prevalence of SMX direct photolysis would be represented by waters that contain at the same time low DOC (< 2 mgC L^{-1}) and high values of nitrate (≥1 mM) and/or nitrite (≥10 μM). In these cases, $CO_3^{\bullet-}$ and $^\bullet$OH would be the main SMX photoreaction pathways. However, such environments are relatively rare and they are often found either in mountain settings strongly affected by atmospheric nitrogen depositions (excluded from the present study), or in the presence of extensive inputs of nitrogen species from contaminated groundwater [36].

It is interesting to compare the predicted lifetimes of SMX with those of sulfadiazine, another sulfonamide antibiotic, under identical model calculations and environmental conditions [42]. The structural difference between the two compounds is that sulfadiazine has a 6-atom heterocyclic ring, whereas SMX has a 5-atom heterocyclic ring. When d = 5 m, the neutral form of sulfadiazine (pKa = 6.5) has $t_{½}$ = 10–15 days for DOC = 2–10 mgC L^{-1} [42]. In the same conditions, anionic sulfadiazine has $t_{½}$ = 10–45 days. Interestingly, anionic sulfadiazine mainly reacts by direct photolysis, while the neutral form would mainly react with ^{3}CDOM* [42]. Comparison of these results with those in Fig. 2 suggests that anionic SMX would be degraded much faster (by almost an order of magnitude) compared to anionic sulfadiazine, with prevalence of direct photolysis in both cases. Anionic SMX would also be degraded a bit faster than neutral sulfadiazine that, however, follows a different photoreaction pathway (reaction with ^{3}CDOM*). Interestingly, significant triplet-sensitization processes are reported for other sulfa drugs with 6-atom heterocyclic rings (sulfamethazine, sulfamerazine, and sulfachloropyridazine), in addition to sulfadiazine [43].

Similarly to sulfadiazine, the neutral form of SMX is also more photolabile than the anionic one [12], but the pKa value of neutral SMX (5.6) makes it less environmentally significant than neutral sulfadiazine. The comparison suggests that SMX is more photolabile than sulfadiazine, and there is evidence that other sulfa drugs with a 5-atom heterocyclic ring (sulfisoxazole, sulfamethizole, sulfathiazole, and sulfamoxole) can be even more photolabile than SMX [10]. Therefore, a 5-atom ring (e.g., SMX) seems to favor photolability of sulfa drugs, while a 6-atom ring (e.g., sulfadiazine) could make the drugs more photostable.

3.2. Assessment of SMX photodegradation on a wide geographic scale

The determination of the equivalent wavelength for the direct photolysis of SMX yielded λ_{eq} = 430 nm. As shown in Fig. 3, the monochromatic approach (dashed curves, obtained using Eq. 12 with η_{SMX} = 9.5 mol E^{-1} nm) closely approximated the polychromatic data (solid squares, obtained with Eq. 11 and Φ_{SMX} = 0.029 mol E^{-1} that is representative of SMX under simulated sunlight [13,14]). This indicates that the monochromatic approximation to the direct photolysis of SMX does not result in a loss of accuracy and supports its use when predicting SMX photoreaction kinetics. Notably, the good agreement is maintained across a wide DOC interval (up to 25 mgC L^{-1}), and for water depths ranging from shallow to deep. Also note that Φ_{SMX} is reported to be independent of the wavelength [13].

The ability of Eqs. (13,14), which are based on the solar-noon photon flux density of sunlight at λ_{eq}, to predict the daily dose G_{day} reaching the ground at mid-latitude (45°N) is illustrated in Fig. 4 for the different

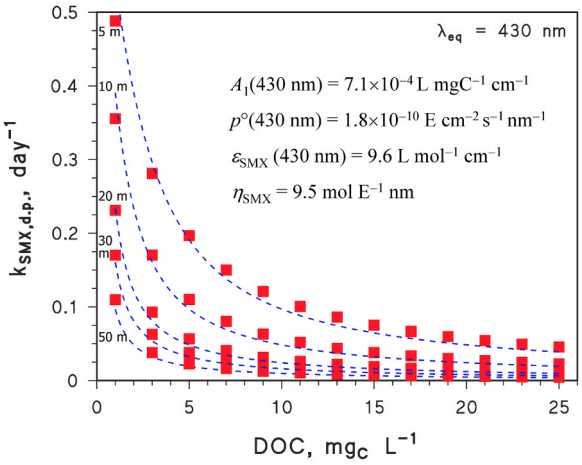

Fig. 3. Direct photolysis rate constants of SMX ($k_{SMX,d.p.}$) in mid-latitude, mid-July and fair-weather conditions, for different values of water depth (5–50 m) and of the DOC. Solid squares: polychromatic calculations (Eq. 11). Dashed curves: monochromatic approximation with λ_{eq} = 430 nm (Eq. 12).

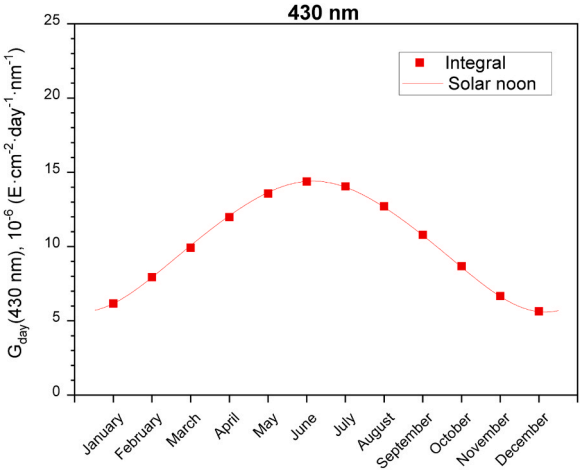

Fig. 4. Daily dose G_{day} reaching the ground at mid-latitude (45°N, λ_{eq} = 430 nm). Solid squares: $G_{day}(\lambda_{eq}) = \int_{1\ day} p^{\circ}(\lambda_{eq}, t)\, dt$. Solid curve: $G_{day}(\lambda_{eq}) = F_1\, p_{sn}^{\circ}(\lambda_{eq})\, \tau_{DL}$, with $F_1 = 0.75$.

months of the year. Excellent agreement was obtained between integrated values (solid squares) and the solar-noon-based estimate (solid curve) by using $F_1 = 0.75$, with a root mean square error (RMSE) of 2.7%.

The same F_1 value was also appropriate to predict G_{day} in the 60°S–60°N latitude belt, as shown in Fig. 5. In this case, the typical RMSE values ranged between 3% and 6%, with higher values (8–11%) observed at the extreme northern and southern latitudes (60°N, 60°S).

The above discussion suggests that it is appropriate to use Eq. (12) to predict the direct photolysis kinetics of SMX, with: $\tau = 480\ \arccos(-\tan(\varphi)\ \tan(\delta))$; $p^{\circ}(430\ nm) = 0.75\ p_{sn}^{\circ}(430\ nm)$, and $p_{sn}^{\circ}(430\ nm)$ as described by Eq. (14) as a function of latitude and the day of the year.

The photodegradation kinetics of SMX was assessed by taking into account both the direct photolysis (d.p.) and the ^{3}CDOM* reaction, as follows (with $k_{SMX,d.p.}$ given by Eq. 12):

$$k_{SMX} = k_{SMX,d.p.} + k_{SMX,^3CDOM^*}[^3CDOM^*]\frac{1}{1+\frac{DOC}{[DOM]_{1/2}}} \quad (15)$$

The values of $k_{SMX,^3CDOM^*}$ and $[DOM]_{½}$ are shown in Table 1.

Note that $[DOM]_{½} = 1.3\ mgC\ L^{-1}$ was used in Eq. (15), but this value would vary depending on the type and source of the DOM [7,18].

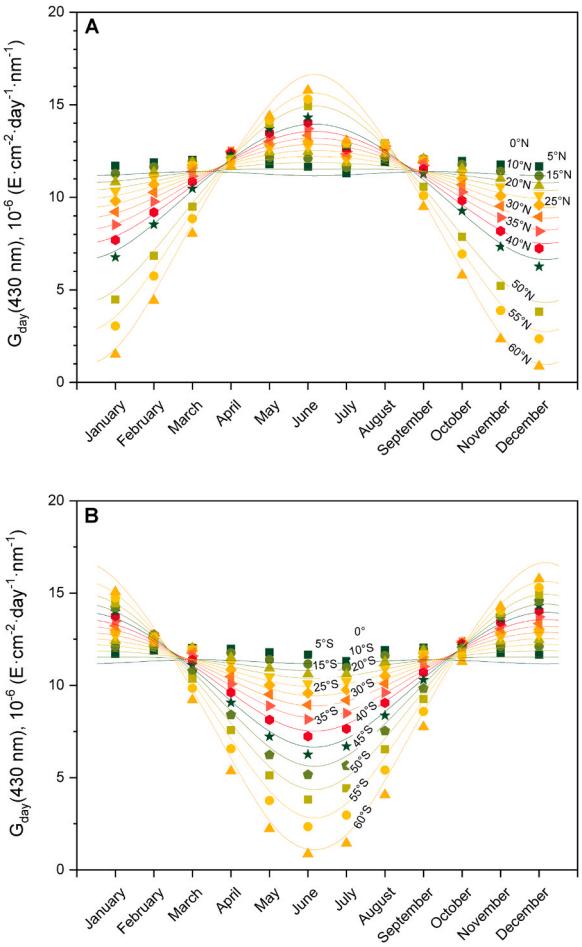

Fig. 5. Validation of the procedure to calculate the daily dose as a function of the latitude and the day of the year (curves: calculated daily dose; dots: integrated daily dose). (A) Latitudes from 0° to 60°N with steps of 5°. (B) Latitudes from 60°S to 0°.

However, considering that triplet sensitization would typically account for < 10% of SMX photodegradation, due to the prevalent role of the direct photolysis, halving or doubling the value of $[DOM]_{½}$ would modify k_{SMX} by no more than 1–1.5%.

The values of [^{3}CDOM*] in worldwide lakes located within 60°S–60°N latitudes have been determined in previous work [26]. In that case as well, a monochromatic photon efficiency for ^{3}CDOM* generation has been identified (λ_{eq} = 560 nm). Calculations based on the daily dose G_{day} have yielded $F_1 = 0.82$ for ^{3}CDOM*, which was appropriate for use in the whole 60°S–60°N latitude belt. The calculated values of [^{3}CDOM*] have been used to predict the photochemical lifetimes of clofibric acid, which mainly undergoes triplet sensitization [26], with good agreement with the available field data (lifetime of clofibric acid in the Swiss Greifensee [41]).

On this basis, Eq. (15) was used to calculate the values of k_{SMX} for each lake, averaged over the year. Afterwards, it was derived $t_{½}(SMX) = \ln 2\ k_{SMX}^{-1}$. The resulting $t_{½}(SMX)$ data (year averages) are shown in Fig. 6. They suggest that: *(i)* SMX is quite photolabile in lake water, with lifetimes of some days (25th percentile 1.7 days; median 2.3 days; 75th percentile 3.2 days); *(ii)* the shortest SMX lifetimes are found in the tropical belt, where generally high sunlight irradiance and relatively low DOC values both favor the direct photolysis of SMX. In contrast, longer lifetimes are usually predicted near 60°N latitude, due to the combination of lower irradiance and higher DOC values [27].

The latitude trend of fair-weather SMX lifetimes is comparable to that of the non-steroidal anti-inflammatory drug diclofenac, which is

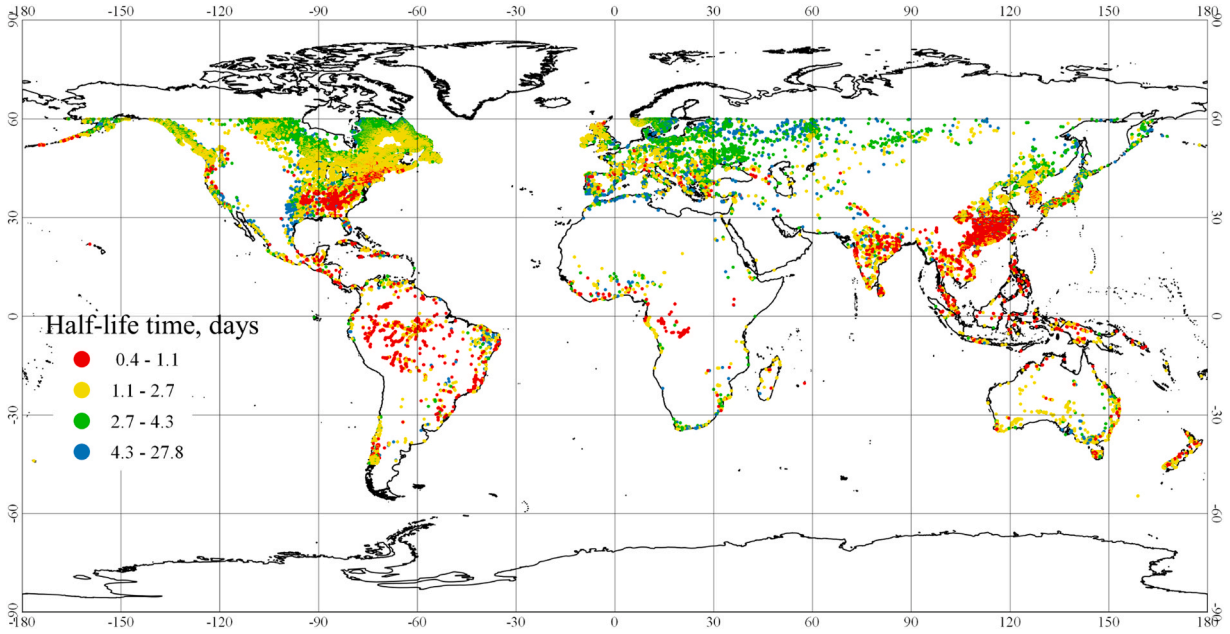

Fig. 6. Global map of the photochemical half-life times of SMX (year averages). Given the depth range of the monochromatic approximation (see Fig. 3), in the case of lakes deeper than 50 m (<1% of the total), it was assumed $d = 50$ m. Note that waters below 50 m depth would be in the dark.

another photolabile pharmaceutical that mainly undergoes photodegradation by direct photolysis. In the case of diclofenac, as well, degradation would be faster in the tropical belt and slower at high Nordic latitudes. However, the predicted lifetimes for SMX are 4–5 times shorter than those of diclofenac under comparable conditions [27].

The above discussion is relevant to cloudless sky, while cloud cover would decrease irradiance [40] and proportionally increase SMX lifetimes. According to available data of actual weather conditions, correction factors for the cloud cover would be quite relevant in some areas of the world [40]. Compared to sunny-sky predictions, SMX lifetimes would be approximately doubled in equatorial areas in South America, Africa and Asia, as well as in South-Eastern China. Note that these are the world regions with the shortest sunny-sky SMX lifetimes (see Fig. 6), thus SMX would still undergo very fast photodegradation. Above 40°N latitude, lifetimes would be increased by 25–30% in North America as well as in Europe and Asia. In these regions, the longest sunny-sky SMX lifetimes are predicted, and cloud cover would make them a bit longer. A similar 25–30% correction applies to the South-Eastern US, where, however, sunny-sky lifetimes would be very short. While increasing SMX lifetimes, consideration of actual weather conditions [40] would not change the prediction that SMX is a photolabile compound.

An additional factor that would make SMX photodegradation less efficient in the tropical belt is lake stratification, which is typically more common and longer-lasting in tropical regions compared to temperate ones [36]. In contrast, winter ice cover that suppresses photoreactions is more likely at elevated northern and southern latitudes than in tropical areas.

The calculated lifetimes of SMX in lake water are a function of DOC, depth, and the latitude φ. Using Eq. (15) to predict SMX photodegradation kinetics is not straightforward, given the calculation procedures needed to obtain $k_{SMX,d.p.}$ and [^{3}CDOM*]. For this reason, a more manageable algebraic function was derived to more easily reproduce the results shown in Fig. 6, with robust performance (R^2 of 0.994, as explained in **Section 2.2.1**). Such an equation reads as follows (note that $t_{½}$(SMX) has [day] units, DOC is in [mgC L^{-1}], d in [m], and φ in degrees; latitude is negative for the Southern hemisphere):

$$t_{½}(\mathrm{SMX}) = 0.25 + 0.0022\,d - 0.135\,\mathrm{DOC} - 0.0039\,\varphi + 0.0021\,\varphi\,\mathrm{DOC} + 0.057\,d\,\mathrm{DOC} + 0.0029\,\mathrm{DOC}^2 - 6.9\times10^{-4}\,d^2 - 8.8\times10^{-5}\,\mathrm{DOC}^3 + 6.9\times10^{-6}\,d^3 \quad (16)$$

The 95% confidence intervals of the coefficients for each variable or combination of variables in Eq. (16) are provided in Table S1 within the Supplementary Material, together with the standardized regression coefficients. The standardized coefficients allow for a more direct interpretation of the effects of DOC, depth, and latitude on the modeled response (lifetime), as the original coefficients shown in Eq. (16) are influenced by the scales, units of measurement, and the non-linear transformations of the three considered variables. The standardized coefficients highlight the importance of DOC, d, and their combinations in $t_{½}$(SMX).

Finally, to ensure the reliability of the predictions and avoid extrapolations outside the original training domain, it is recommended to use Eq. (16) within its range of applicability: sunny weather, well-mixed water, latitude between 60°S and 60°N, DOC between 0.3 and 23 mgC L^{-1}, and depth between 5 and 50 m.

4. Conclusions

Direct photolysis is expected to be the main phototransformation pathway of SMX in sunlit freshwaters, making SMX rather photolabile in well-mixed waters under clear-sky conditions. Cloudy sky, water stratification, and ice cover would make SMX photodegradation less efficient.

Phototransformation kinetics are affected by environmental factors such as sunlight irradiance and, among water parameters, primarily depth and DOC. In particular, the predicted SMX photodegradation is faster under high irradiance, low water depth (deep waters are poorly illuminated by sunlight), and low DOC conditions (dissolved organic compounds compete with SMX for the absorption of solar radiation). In very shallow waters, the predicted lifetime of SMX (hours to a day) aligns with results from several irradiation experiments reported in the literature, which also used low water depths.

For lakes situated across a broad geographic range the photodegradation of SMX is again predicted to be quite rapid, with lifetimes in the range of days to some weeks in well-mixed waters under clear-sky conditions. This is especially true in the tropical belt, where average

annual irradiance is high and the DOC values of lake waters are generally lower than, for instance, in elevated boreal latitudes. Effects of cloudy sky could make average lifetimes longer by 25–30% (e.g., South-Eastern US and regions above 40°N latitude in North America, Europe, and Asia), or even double compared to clear-sky predictions (equatorial regions, South-Eastern China), but it is still suggested that SMX would be a photolabile compound.

A practical algebraic function (Eq. 16) can be identified that closely fits the predictions of SMX lifetime in well-mixed and sunlit lake waters, as a function of depth (5–50 m), DOC (0.3–23 mgC L^{-1}), and latitude (60°S−60°N).

CRediT authorship contribution statement

Luca Carena: Writing – review & editing, Validation, Supervision, Investigation, Data curation. **Sara Abdelli:** Writing – review & editing, Writing – original draft, Investigation, Data curation. **Davide Ballabio:** Writing – review & editing, Supervision, Methodology, Conceptualization. **Enmanuel Cruz Muñoz:** Writing – review & editing, Writing – original draft, Investigation, Data curation. **Paola Calza:** Writing – review & editing, Validation, Supervision, Funding acquisition. **Ángela García-Gil:** Writing – review & editing, Writing – original draft, Investigation, Data curation. **Davide Vione:** Writing – review & editing, Writing – original draft, Validation, Software, Project administration, Conceptualization. **Laura Ferrando-Climent:** Writing – review & editing, Validation, Supervision, Project administration, Methodology. **Viviana Consonni:** Writing – review & editing, Validation, Software, Formal analysis, Data curation. **Javier Marugán:** Writing – review & editing, Validation, Supervision, Resources, Conceptualization. **Roberto Todeschini:** Writing – review & editing, Validation, Supervision, Software.

Declaration of Competing Interest

The authors declare the following financial interests/personal relationships which may be considered as potential competing interests: Javier Marugán serves as Editor of the Journal of Environmental Chemical Engineering. The editorial handling and review of this manuscript were managed by a different and independent Editor. If there are other authors, they declare that they have no known competing financial interests or personal relationships that could have appeared to influence the work reported in this paper.

Acknowledgements

This research was supported by the European Union under the Marie Skłodowska-Curie Actions (MSCA) – Doctoral Network- IN2AQUAS (grant agreement No. 101119555) and by MSCA-Horizon 2020-RISE SusWater (grant agreement No. 101007578). LC, PC, and DV also acknowledge support from the Project CH4.0 under the MUR Program "Dipartimenti di Eccellenza 2023–2027" (CUP: D13C22003520001).

Supplementary material available

A text, machine-readable version of Eq. (16). Table S1, reporting the coefficients for each variable or combination of variables in Eq. (16) and their 95% confidence intervals, together with the standardized regression coefficients.

Appendix A. Supporting information

Supplementary data associated with this article can be found in the online version at doi:10.1016/j.jece.2026.124441.

Data availability

Data will be made available on request.

References

[1] S.D. Richardson, T. Manasfi, Water analysis: Emerging contaminants and current issues, Anal. Chem. 96 (2024) 8184–8219.
[2] F. Riva, E. Zuccato, C. Pacciani, A. Colombo, S. Castiglioni, A multi-residue analytical method for extraction and analysis of pharmaceuticals and other selected emerging contaminants in sewage sludge, Anal. Methods 13 (2021) 526–535.
[3] I.O. Sanusi, G.O. Olutona, I.G. Wawata, H. Onohuean, Occurrence, environmental impact and fate of pharmaceuticals in groundwater and surface water: a critical review, Environ. Sci. Pollut. Res. 30 (2023) 90595–90614.
[4] W.L. Desiante, N.S. Minas, K. Fenner, Micropollutant biotransformation and bioaccumulation in natural stream biofilms, Water Res. 193 (2021) 116846.
[5] Z. Guo, D. Kodikara, L.S. Albi, Y. Hatano, G. Chen, C. Yoshimura, J. Wang, Photodegradation of organic micropollutants in aquatic environment: Importance, factors and processes, Water Res. 231 (2023) 118236.
[6] D. Vione, A. Scozzaro, Photochemistry of surface fresh waters in the framework of climate change, Environ. Sci. Technol. 53 (2019) 7945–7963.
[7] K. McNeill, S. Canonica, Triplet state dissolved organic matter in aquatic photochemistry: reaction mechanisms, substrate scope, and photophysical properties, Environ. Sci. Process. Impacts 18 (2016) 1381–1399.
[8] R. Ossola, O.M. Jönsson, K. Moor, K. McNeill, Singlet oxygen quantum yields in environmental waters, Chem. Rev. 121 (2021) 4100–4146.
[9] A.C. Johnson, V. Keller, E. Dumont, J.P. Sumpter, Assessing the concentrations and risks of toxicity from the antibiotics ciprofloxacin, sulfamethoxazole, trimethoprim and erythromycin in European rivers, Sci. Total. Environ. 511 (2015) 747–755.
[10] A.L. Boreen, W.A. Arnold, K. McNeill, Photochemical fate of sulfa drugs in the aquatic environment: sulfa drugs containing five-membered heterocyclic groups, Environ. Sci. Technol. 38 (2004) 3933–3940.
[11] A.G. Trovó, R.F. Nogueira, A. Agüera, C. Sirtori, A.R. Fernández-Alba, Photodegradation of sulfamethoxazole in various aqueous media: persistence, toxicity and photoproducts assessment, Chemosphere 77 (2009) 1292–1298.
[12] C. Oliveira, D.L.D. Lima, C.P. Silva, V. Calisto, M. Otero, V.I. Esteves, Photodegradation of sulfamethoxazole in environmental samples: The role of pH, organic matter and salinity, Sci. Total. Environ. 648 (2019) 1403–1410.
[13] W.U. Palm, N. Schmidt, M. Stahn, S. Grimme, A kinetic study of the photolysis of sulfamethoxazole with special emphasis on the photoisomer, Photochem. Photobiol. Sci. 22 (2023) 615–630.
[14] M.A. Andino-Enríquez, D. Fabbri, D. Vione, P. Calza, Photoinduced transformation pathways of the sulfonamide antibiotic sulfamethoxazole, relevant to sunlit surface waters, Environ. Pollut. 384 (2025) 126947.
[15] E.C. Muñoz, D. Ballabio, V. Consonni, R. Todeschini, L. Carena, I. Sciscenko, S. Canonica, M. Minella, D. Vione, Photochemical degradation of the aromatic amine 4-(N,N-dimethylamino)benzonitrile: Triplet, sensitisation back Reduct. (quasi−)Glob. Model. J. Environ. Chem. Eng. 14 (2026) 121537.
[16] D. Vione, A critical view of the application of the APEX software (Aqueous Photochemistry of Environmentally-occurring Xenobiotics) to predict photoreaction kinetics in surface freshwaters, Molecules 25 (2020) 9.
[17] S. Garg, T.D. Waite, Is singlet oxygen an important oxidant in advanced oxidation processes? Environ. Sci. Technol. 59 (2025) 26320–26341.
[18] J. Wenk, U. von Gunten, S. Canonica, Effect of dissolved organic matter on the transformation of contaminants induced by excited triplet states and the hydroxyl radical, Environ. Sci. Technol. 45 (2011) 1334–1340.
[19] S.E. Braslavsky, Glossary of terms used in photochemistry 3rd edition, Pure Appl. Chem. 79 (2007) 293–465.
[20] R. Cela Torrijos, R. Phan-Tan-Luu, 1.09 - Introduction Experimental Designs, in: S. Brown, R. Tauler, B. Walczak (Eds.), Comprehensive Chemometrics (Second Edition), Elsevier, 2020, pp. 205–208.
[21] N.R. Draper, H, Smith. Applied Regression Analysis, 3rd Edition, Wiley, New York, 1998.
[22] U. Grömping, Variable importance in regression models, WIREs Comput. Stat. 7 (2015) 137–152.
[23] K. Toming, J. Kotta, E. Uuemaa, S. Sobek, T. Kutser, L.J. Tranvik, Predicting lake dissolved organic carbon at a global scale, Sci. Rep. 10 (2020) 8471.
[24] M.L. Messager, B. Lehner, G. Grill, I. Nedeva, O. Schmitt, Estimating the volume and age of water stored in global lakes using a geo-statistical approach, Nat. Commun. 7 (2016) 13603.
[25] NCAR, Quick T.U.V. calculator [WWW Document] (2015) URL http://cprm.acom.ucar.edu/Models/TUV/Interactive_TUV/.
[26] L. Carena, Á. García-Gil, J. Marugán, D. Vione, Global modeling of lake-water indirect photochemistry based on the equivalent monochromatic wavelength approximation: The case of the triplet states of chromophoric dissolved organic matter, Water Res. 24 (2023) 120153.
[27] L. Carena, Á. García-Gil, J. Marugán, D. Vione, Global modeling of photochemical reactions in lake water: A comparison between triplet sensitization and direct photolysis, Eco-Environ. Heal. 4 (2025) 100123.
[28] D. Vione, The modelling of surface-water photoreactions made easier: introducing the concept of 'equivalent monochromatic wavelengths', Water Res. 190 (2021) 116675.

[29] Á. García-Gil, J. Marugán, D. Vione, A model to predict the kinetics of direct (endogenous) virus inactivation by sunlight at different latitudes and seasons, based on the equivalent monochromatic wavelength approach, Water Res. 208 (2022) 117837.
[30] National Renewable Energy Laboratory, Solar Position Algorithm| NREL. [WWW Document] (2026).
[31] J. Moreno-SanSegundo, S. Giannakis, S. Samoili, G. Farinelli, K.G. McGuigan, J. Marugán, SODIS potential: a novel parameter to assess the suitability of solar water disinfection worldwide, Chem. Eng. J. 419 (2021) 129889.
[32] QGIS.org. QGIS Geographic Information System. QGIS Association. http://www.qgis.org (2026).
[33] F. Calderaro, D. Vione, Possible effects of climate change on surface-water photochemistry. A model assessment of the impact of browning on the photodegradation of pollutants in lakes during summer stratification: Epilimnion vs. whole-lake phototransformation, Molecules 25 (2020) 2795.
[34] J.N. Apell, S. Kliegman, C. Solá-Gutiérrez, K. McNeill, Linking triclosan's structural features to its environmental fate and photoproducts, Environ. Sci. Technol. 54 (2020) 14432–14441.
[35] S.A. Loiselle, H. Duan, Z. Cao, Characteristics of the underwater light field, in: P. Calza, D. Vione (Eds.), Surface Water Photochemistry, The Royal Society of Chemistry, 2015, pp. 39–59. Ch. 3.
[36] R.G. Wetzel. Limnology: Lake and River Ecosystems, Third. ed, Academic Press, 2001.
[37] S.F. Jane, L.A. Winslow, C.K. Remucal, K.C. Rose, Long-term trends and synchrony in dissolved organic matter characteristics in Wisconsin, USA, lakes: Quality, not quantity, is highly sensitive to climate, J. Geophys. Res. Biogeosci. 122 (2017) 546–561.
[38] G. McKay, W. Huang, C. Romera-Castillo, J.E. Crouch, F.L. Rosario-Ortiz, R. Jaffé, Predicting reactive intermediate quantum yields from dissolved organic matter photolysis using optical properties and antioxidant capacity, Environ. Sci. Technol. 51 (2017) 5404–5413.
[39] B. Koehler, T. Landelius, G.A. Weyhenmeyer, N. Machida, J.J. Tranvik, Sunlight-induced carbon dioxide emissions from inland waters, Glob. Biogeochem. Cycles 28 (2014) 696–711.
[40] S.B. Partanen, K. McNeill, Global corrections to reference irradiance spectra for non-clear-sky conditions, Environ. Sci. Technol. 57 (2023) 2682–2690.
[41] C. Tixier, H.P. Singer, S. Oellers, S.R. Müller, Occurrence and fate of carbamazepine, clofibric Acid, diclofenac, ibuprofen, ketoprofen, and naproxen in surface waters, Environ. Sci. Technol. 37 (2003) 1061–1068.
[42] D. Vione, D. Fabbri, M. Minella, S. Canonica, Effects of the antioxidant moieties of dissolved organic matter on triplet-sensitized phototransformation processes: Implications for the photochemical modeling of sulfadiazine, Water Res. 128 (2018) 38–48.
[43] A.L. Boreen, W.A. Arnold, K. McNeill, Triplet-sensitized photodegradation of sulfa drugs containing six-membered heterocyclic groups: Identification of an SO_2 extrusion photoproduct, Environ. Sci. Technol. 39 (2005) 3630–3638.